Inverted Flexible Pavement Response and Performance

EROL TUTUMLUER AND RICHARD D. BARKSDALE

An inverted section consists of an unstabilized crushed-stone base sandwiched between a lower cement-stabilized layer and the upper asphalt concrete (AC) surfacing. Two inverted full-scale instrumented pavement sections were tested to rutting or fatigue failure in a laboratory facility. One inverted section had a 152-mm (6-in.) cement-stabilized crushed-stone subbase and the other a 152-mm (6-in.) cement-treated silty sand subbase. The inverted sections were loaded up to 4.4 million load repetitions at failure. A 28.9-kN (6,500-lb) uniform circular loading was applied to the surface and systematically moved to prevent a punching failure. The inverted sections exhibited better performance compared to conventional and full-depth AC sections also tested. The inverted sections had lower vertical stresses on the subgrade and lower resilient surface deflections than the other sections. The rigid cement-stabilized subbase was effective in bridging a weak subgrade. The inverted section made optimum use of the compressive characteristics of the unstabilized aggregate base where stresses were compressive. A nonlinear finite-element program, GT-PAVE, was used to calculate the resilient pavement response. GT-PAVE did a reasonable job of simultaneously predicting the measured deformation and stress and strain response at six points in the different layers of the inverted sections. A sensitivity analysis indicates the use of a 152-mm (6-in.) unstabilized aggregate base and a 152- to 203-mm-thick (6- to 8-in.) cement-stabilized subbase to be an attractive inverted section design.

Today, more than 3.5 million km (2.2 million mi) of paved roads exist in the United States of which 94 percent consist of flexible pavements (*1*). Most of these flexible pavements have unstabilized aggregate bases or subbases. To achieve maximum economy in a pavement section, each material, including the unstabilized aggregate base, should be located to take full advantage of its best engineering properties. An inverted section consists of unstabilized aggregate base sandwiched between a lower cement-stabilized subbase and the upper asphalt concrete surfacing. An inverted section offers an interesting alternative to conventional flexible pavements with the inverted section making optimal use of the properties of each material.

This paper describes the behavior of two full-size inverted sections having (a) a cement-treated silty sand subbase and (b) a cement-stabilized aggregate subbase. These sections, as well as conventional ones, were constructed in the laboratory under carefully controlled conditions and tested to failure under cyclic loading. Stresses, strains, and deflections were measured at a number of locations in the different layers of the sections. A nonlinear finite-element program, GT-PAVE, was used to calculate pavement response and compare the theoretical values with the observed deformations, stresses, and strains. Pavement performance of the inverted sections was also directly compared with conventional and full depth asphalt concrete (AC) sections.

School of Civil and Environmental Engineering, Georgia Institute of Technology, Atlanta, Ga. 30332.

PREVIOUS STUDIES

The performance of inverted highway test sections has been reported in works by Johnson (*2*), and McGhee (*3*). An inverted test section subjected to aircraft loadings was studied (*4*). These inverted sections have all demonstrated good performance. On the basis of a 5-year study, an inverted section was found to be the most effective design and to exhibit the lowest overall cost of the sections included in the study (*3*). The subbase was constructed by stabilizing a residual micaceous silt and clayey silt subgrade with 10 percent cement by volume.

North Carolina State University researchers have recently found that among 24 full-scale flexible pavements tested, inverted sections having cement stabilized subgrades performed the best. These sections had unstabilized aggregate bases approximately 203 to 305 mm thick (8 to 12 in.) overlain by a 178-mm (7-in.) thick soil-cement subbase.

Asphalt concrete surface thicknesses of inverted sections have been relatively thin, varying from 38 to 76 mm (1.5 to 3 in.). The unstabilized aggregate base used in inverted sections has typically varied from 152 to 203 mm (6 to 8 in.) in thickness. A base having this range of thickness is relatively effective in eliminating or reducing reflection cracking. The subbase of two inverted highway sections (*2,3*) have both been 152 mm (6 in.) thick. The importance of using a high-quality cement-stabilized layer has been demonstrated through field performance (*5*).

Inverted sections are attractive in areas of low rainfall where there is no potential problem of water being trapped in the base above the low-permeability cement-stabilized layer. The successful use of inverted sections in Virginia (*3*), which is in a high rainfall area, suggests water being trapped in the base may not be a significant problem. When water is of concern, a free-draining base with provision for positive water collection should be provided.

The works of Maree et al. (*6,7*) and that of O'Neil et al. (*8*) have shown that an unstabilized aggregate layer, when confined in an inverted section or a granular overlay, develops large elastic moduli as high as 689 MPa (100 ksi). Criteria to give optimum performance for the unstabilized aggregates used in inverted sections have been developed (*9*). It was also found that an unstabilized aggregate layer, when used in an overlay between the old pavement and the resurfacing, reduces reflection cracking, which substantiates earlier experience in Arkansas (*8*).

The degree of saturation of an inverted section base has been found to increase because of cracks that form in the cement stabilized layer due to shrinkage or fatigue, or both (*7,9*). Rutting becomes greater and the elastic moduli decrease with the increase in base saturation. Even in wet conditions, a high-quality, well-constructed crushed-aggregate base, when used in an inverted section, is still quite resistant to rutting (*7,9*), with rutting in one instance observed to be one-half that of a conventional section (*9*).

MATERIAL PROPERTIES

The aggregate gradations and material properties used in the inverted test sections are summarized in Table 1. A Georgia Department of Transporation (DOT) B-binder asphalt concrete was used for the AC surfacing. The asphalt cement used in the mix was an AC-20 viscosity grade. The unstabilized aggregate base course consisted of crushed granitic gneiss prepared by blending in a small 0.096-m^3 (1/8-yd^3) Barber-Greene pugmill 20 percent by weight of No. 5 size aggregate, 25 percent of No. 57, and 55 percent of No. 810s. A low to moderate strength micaceous nonplastic silty sand subgrade, classified as an AASHTO A-4 soil, was used beneath the inverted test sections.

Equation 1 gives the observed resilient modulus variation as a function of bulk stress and deviator stress obtained from repeated load triaxial tests performed on the unstabilized aggregate base (*10*).

$$M_R(\text{MPa}) = 543.82\ \sigma_\theta^{0.61}\ \sigma_d^{-0.07} \quad r^2 = 0.95 \tag{1}$$

The foregoing resilient modulus model proposed in a work by Uzan (*11*) gives a much better fit of resilient modulus than does the more familiar K-θ model.

The nonlinear behavior of the silty sand subgrade was modeled using a bilinear approximation to give resilient modulus as a function of deviator stress (σ_d). The measured resilient modulus M_R (*12*), when corrected for soil suction effects, was as follows: $\sigma_d = 0$, M_R = 241 325 kPa (35,000 psi); σ_d = 17.2 kPa (2.5 psi), M_R = 40 681 kPa (5,900 psi), and σ_d = 68.9 kPa (10 psi), M_R = 39 302 kPa (5,700 psi).

INVERTED TEST SECTION CONSTRUCTION

Pavement testing was conducted in a facility consisting of a 2.4-m (8-ft) by 36.6-m (12-ft) in plan and 1.5-m (5-ft)-deep test pit. Cyclic load was applied by an air over oil pneumatic loading system attached to a heavy steel load frame. A 28.9-kN (6,500-lb) uniform dynamic load was applied to the surface of the test sections over a diameter of 231 mm (9.1 in.). Twelve large-scale pavement test sections were tested to evaluate pavement performance (*12*). Pavements tested in this facility consisted of two inverted sections, five conventional sections having crushed-stone bases, and five full-depth asphalt concrete sections (Table 2).

The two inverted test sections (Section 11 and Section 12, Table 2) consisted of 203 mm (8 in.) of unstabilized crushed-stone base sandwiched between 89 mm (3.5 in.) of asphalt concrete above and 152 mm (6 in.) of cement stabilized material below. The silty sand subgrade beneath the cement-stabilized subbase was 1118 mm (44 in.) deep. A concrete slab was located beneath the subgrade.

The silty sand subgrade was placed in 51-mm (2-in.) lifts up to a total thickness of 1 118 mm (44 in.) in the inverted sections. Each lift was compacted using a Wacker or a Jay 12 compactor to 98 percent of AASHTO T-99 standard proctor maximum dry density at a moisture content of 20.5 percent. A spring-loaded static penetrometer was used to ensure uniformity of the subgrade during construction. As-constructed density was determined using a thin wall drive tube sampler.

The 152-mm-(6-in.) thick cement-stabilized subbase of the inverted sections was constructed on top of the subgrade followed by the placement of the crushed-stone base. Base and subbase layers were placed in approximately 51-mm (2-in.) lifts. Compaction of the subbase and base was achieved using five to seven passes of the Jay 12 vibrating plate compactor. The unstabilized aggregate bases were compacted to 100 percent of the AASHTO T-180 modified proctor maximum dry density. Nuclear density measurements revealed that because of the presence of the underlying rigid cement-stabilized subbase, the compaction density in the unstabilized aggregate base was 105 percent of the T-180 maximum dry density.

The cement-stabilized layers were cured for 28 days. The B-binder asphalt concrete mix was then placed over the unstabilized base. The B-binder gives a strong asphalt concrete surface course to resist rutting in that layer under the heavy applied loading.

INVERTED TEST SECTION RESULTS

The full-scale laboratory tests conducted to failure permitted comparing the performance of the inverted sections with the full-depth asphalt concrete sections and the conventional sections having relatively thick layers of unstabilized crushed aggregate base (Tables 2 and 3). Test results for the conventional aggregate base and full-depth asphalt concrete sections have been previously described, as well as the instrumentation and loading scheme used in the study (*12,13*). A fatigue failure of the test sections was considered to occur when the surface cracks connected to form a grid-type pattern, usually over the loaded area. Only hairline cracks were allowed to develop. Before wider cracks formed, testing was terminated because of the large number of repetitions required to reach this state of deterioration.

A maximum rut depth of 13 mm (0.5 in.) was considered to constitute a rutting failure. The maximum rut depth was determined by averaging the rut depths measured at completion of testing at the primary load position and at completion of testing at the sixth secondary load position. The need for averaging the values of rutting was because of the varying amounts of creep and plastic flow of the asphalt concrete and base materials observed at the different load positions as the load was moved from one position to another.

Overall, the two inverted sections performed the best of all the sections studied (Table 2). The cement-stabilized crushed-stone subbase inverted section (Section 12) failed in combined fatigue and rutting after 4.4 million load repetitions, making it clearly the strongest section. The cement-treated silty sand subbase inverted section (Section 11) withstood 3.6 million repetitions giving this section the next best performance. The two inverted sections also exhibited lower vertical stress on the subgrade and lower resilient surface displacements than the other sections (Table 3).

The cement-treated silty sand subbase inverted section appeared to perform slightly better than the conventional 305-mm (12-in.) thick crushed-stone base section (Section 1), which failed at an estimated 3.5 million repetitions. Both sections had 89-mm (3.5-in.) AC surfacing. The inverted section, however, had a 203-mm (8-in.) crushed-stone base and 152-mm (6-in.) cement-treated subbase.

The performance of one section compared to another section is directly dependent on the specific properties of each section. Rutting failure of the asphalt concrete section occurred, to a significant extent, within the asphalt concrete. The asphalt concrete, as placed in the test sections, met the specifications for a Georgia DOT mix. Better-performing AC mixes could probably have been identified and used. The results, however, show that when a high-quality unstabilized aggregate base is constructed over a properly prepared subgrade, both the properties and performance of the AC become important and can become the weak link in the design.

TABLE 1 Aggregate Gradations and Material Properties Used In Flexible Pavement Test Sections[1]

SIEVES	Cumulative % Passing By Weight										Maximum Density (kN/m^3)	Opt. Water Content (%)
	38 mm (1.5 in.)	25 mm (1 in.)	19 mm (3/4 in.)	13 mm (1/2 in.)	10 mm (3/8 in.)	4.75 mm (No. 4)	2.00 mm (No. 10)	.425 mm (No.40)	0.25 mm (No. 60)	0.075 mm (No. 200)		
AC Aggregate Gradation: [2]	100	100	100	86	75	51	36	18	14	7	22.9	-
Base Aggregate Gradations:												
No. 5	100	96	37	5	2	-	-	-	-	-	-	-
No. 57	100	98	82	43	20	3	-	-	-	-	-	-
No. 810	100	100	100	100	100	77	56	27	19	8	-	-
Combined [3]	100	99	83	67	61	43	31	15	10	4	21.5 [5]	5.7
Subgrade Gradation:	100	100	100	100	100	100	99	85	70	39	16.5 [4]	18.5
CEMENT STABILIZED SUBBASE PROPERTIES :												
A. Soil - Cement Subbase: 5% by weight of Type I Portland cement added to the silty sand subgrade. (Section 11) Average 28-day unconfined compressive strength = 1476 kPa.											16.8 [5]	18.0
B. Aggregate - Cement Subbase: 4.5% by weight of Type I Portland cement added to the Combined base. (Section 12) Average 28-day unconfined compressive strength = 7902 kPa.											21.7 [5]	6.0

Notes:
1. 1 in. = 25.4 mm; 1 psi = 6.895 kPa; 1 lb = 4.448 kN
2. The B-binder AC had a 5.2% optimum asphalt content, 4 % voids in the total mix, Marshall mix stability of 10.2 kN (2300 lbs.), and a flow value of 2.3 mm (9.0/100.0 in.)
3. Maximum aggregate size = 38 mm
4. Determined by AASHTO T-99 test method
5. Determined by AASHTO T-180 test method

TABLE 2 Geometry and Performance Summary of Pavement Test Sections

Asphalt Concrete Thickness (mm)	Crushed Stone Thickness (mm)	Repetitions to Failure	Failure Mode	Comments
CRUSHED STONE BASE				
89.0	305.0	3,000,000	Fatigue/	
		3,500,000	Rutting	Tested to 2.4 million repetitions
				Failure Extrapolated
89.0	203.0	1,000,000	Rutting	
FULL DEPTH ASPHALT				
229.0	None	10,000,000	Rutting	Bad Asphalt:
			(25 mm)	AC Content: 5.9 %
				Flow: 3.9 mm
165.0	None	10,000	Rutting	Stability: 8318 kN
			(25 mm)	Dry Density: 22.8 kN/m^3
229.0	None	130,000	Rutting	Rutting Primarily in AC
165.0	None	440,000	Rutting	Rutting Primarily in AC
178.0	None	150,000	Rutting	
CRUSHED STONE BASE				
89.0	203.0	550,000	Rutting	
89.0	203.0	2,400,000	Fatigue	Permanent Deformation: 7 mm
89.0	203.0	2,900,000	Fatigue	Permanent Deformation: 9 mm
INVERTED SECTIONS				
89.0	203.0	3,600,000	Fatigue/	152 mm Soil Cement Subbase
			Rutting	
89.0	203.0	4,400,000	Fatigue/	152 mm Cement Stabilized
			Rutting	Subbase

Note: 1 in = 25.4 mm; 1 psi = 6.895 kPa; 1 lb = 4.448 kN

TABLE 3 Detailed Summary of Resilient Test Section Response

Section	Horizontal Tensile Strain (micro m/mm)		Vertical Stress (kPa)		Vertical Strain (micro m/mm)				Surface Deflection (mm)	
	Bottom AC	Bottom Base	Top Base	Top Subgrade	AC	Top Base	Bottom Base	Top Subgrade	254 mm from Centerline	368 mm from Centerline
CRUSHED STONE BASE										
1	0.465	0.597	-	23.4	-	-	-	1.700	0.76	0.38
2	0.674	0.754	-	-	11.000	21.300	-	13.100	0.48	0.25
FULL DEPTH ASPHALT										
3	Premature Failure - Excessive Asphalt Content									
4	Premature Failure - Excessive Asphalt Content									
5	0.319	-	-	60.0	0.850	-	-	1.380	0.30	0.18
6	0.460	-	-	86.9	-	-	-	1.500	0.51	0.30
7	0.410	-	-	88.9	0.650	-	-	2.200	0.48	0.33
CRUSHED STONE BASE										
8	0.300	0.375	-	82.1	-	0.560	0.110	1.850	0.51	0.33
9	0.280	1.080	62.0	76.5	-	0.560	0.340	1.750	0.56	0.33
10	0.400	1.025	54.0	46.9	-	0.620	0.400	2.500	0.43	0.25
INVERTED SECTION										
11	0.340	0.054	-	22.8	-	0.730	0.370	0.390	0.18	0.08
12	0.260	0.022	-	23.4	-	0.760	0.420	0.340	0.15	0.08

Note: "-" in a data field indicates data was not taken.
1 in = 25.4 mm; 1 psi = 6.895 kPa

Horizontal Tensile Strain

The resilient tensile strain occurring in the bottom of an AC surfacing, as shown by laboratory testing and field studies, is related to fatigue life of a flexible pavement. AC surface thickness was held constant in this study, although fatigue life decreases with increasing AC thickness for a given level of tensile strain.

The cement-stabilized crushed-stone subbase section experienced a measured horizontal radial tensile strain of about $260 * 10^{-6}$ mm/mm at the bottom of the AC surfacing. In contrast, the cement-treated silty sand subbase inverted section exhibited a larger horizontal tensile strain of about $340 * 10^{-6}$ mm/mm. The crushed-stone cement-stabilized subbase used in Section 12 was thus more effective in reducing the tensile strain in the asphalt concrete than the less rigid, cement-treated subbase of Section 11.

For comparison with the inverted sections, the tensile strains observed in the bottom of the AC surfacing of the conventional unstabilized aggregate base and full depth AC sections varied from $280 * 10^{-6}$ to $674 * 10^{-6}$ mm/mm with the average measured value being $413 * 10^{-6}$ mm/mm. The tensile strain of $260 * 10^{-6}$ mm/mm observed in the cement-stabilized aggregate subbase inverted section was slightly less than the $280 * 10^{-6}$ mm/mm measured in the best performing noninverted section (Section 1). This finding is in agreement with the observed fatigue performance.

In the inverted sections (Sections 11 and 12), the measured horizontal tensile strains between the crushed-stone base and the cement-treated layer were $54 * 10^{-6}$ and $22 * 10^{-6}$ mm/mm, respectively. These tensile strains were about 20 times smaller than the values measured in the conventional Sections 8, 9, and 10. These small observed strains in the inverted sections were due to the presence of the very stiff subbase beneath the interface at which the strain was measured. The small tensile strains are compatible with the theoretical finding that the lower portion of the unstabilized aggregate base is in a compressive stress state compared to a tensile stress state for a conventional aggregate base section. Because of the compressive stress state, a higher resilient modulus exists in the base of an inverted section than in a conventional base section.

Subgrade Stress

The average measured vertical stress on top of the subgrade of the inverted sections was 22.8 kPa (3.3 psi) for Section 11 and 23.4 kPa (3.4 psi) for Section 12 after 3.6 and 4.4 million load repetitions, respectively (Table 3). These subgrade stresses were up to three times smaller than the vertical stresses measured for the conventional crushed-stone base sections (Sections 8 and 9) and for the full-depth AC sections (Sections 6 and 7). These small vertical subgrade stresses in the inverted sections were caused by the rigid cement stabilized layer bridging the subgrade and greater depth. Section 1, which had the 305-mm (12-in.) thick unstabilized aggregate base and exhibited excellent performance, also had a measured vertical subgrade stress of 23.4 kPa (3.4 psi).

Vertical Displacement

Because a uniform load was applied to the surface using a flexible water-filled bladder, surface deflection could not be measured beneath the load using externally mounted linear variable differential transformers. The closest vertical resilient displacement to the centerline measured in the inverted sections was at a radial distance of 254 mm (10 in.) away from the centerline. Vertical resilient deformations measured in the inverted sections at this location were quite small and varied from 0.15 to 0.18 mm (0.006 to 0.007 in.) (Table 3). These deflections were up to four times smaller than the 0.3 to 0.76 mm (0.012 to 0.03 in.) measured at the same location in the conventional crushed-stone base sections and up to two times smaller than the 1.78 to 0.33 mm (0.07 to 0.013 in.) measured in the full-depth AC sections.

The inverted sections, which had a very rigid cement-stabilized subbase, were also effective in reducing permanent deformation in the subgrade compared to the other test sections. For example, only about 12 percent of the total permanent deformation occurred in the subgrade of the inverted sections compared with 68 percent in the subgrade of the conventional aggregate base sections (Sections 9 and 10). In the inverted sections, about 70 percent of the total permanent deformation occurred in the thin 89-mm (3.5-in.) thick asphalt concrete layer. The remaining 18 percent developed mostly in the upper half of the unstabilized crushed-stone base. The small relative amount of rutting in the base was at least partly because of the very high density obtained in that layer as a result of the presence of the rigid subbase on which the base was compacted. A high level of confinement provided by the rigid layer also accounts for some of the good performance of the crushed-stone base. Based on these findings, the inverted section is particularly attractive for use over a weak subgrade.

PREDICTION OF INVERTED SECTION RESPONSE

The recently developed nonlinear finite-element program GT-PAVE was used to predict the observed pavement resilient response (stresses, strains, and deformations) at different locations in the inverted sections (Table 3). Laboratory-evaluated material properties were used in the theoretical analysis except for the cement-stabilized subbase, which was estimated from correlations given in the literature. After finding reasonably good agreement between the predicted and observed response values in the inverted sections, a sensitivity analysis was performed for selected inverted pavement geometries using materials similar to those in the full-scale test study. The sensitivity analysis permitted determining optimum geometries for inverted sections and extending, at least approximately, the test section results to other conditions.

GT-PAVE Program Capabilities

The GT-PAVE nonlinear computer program uses isoparametric eight-node quadrilateral elements to analyze a flexible pavement as an axisymmetric solid consisting of either linear or nonlinear elastic layers. In the nonlinear elastic layers, a variation in response of the pavement with stiffness occurs as a result of using stress-dependent resilient moduli obtained from the material characterization models. A nonlinear analysis is performed in two stages: first, the gravity and initial stresses are calculated using 5 load increments, and then the wheel load is applied in 10 load increments. The no-tension modification approach in a work by Zienkiewicz et al. (*14*) is used in the granular base when it goes into tension.

Theoretical Analysis

A 140-element, 475-node axisymmetric finite-element mesh was used to analyze both inverted sections as nonlinear elastic layered

systems (Figure 1). The subgrade and the unstabilized aggregate base were treated as nonlinear elastic materials, and the AC surfacing and cement-stabilized subbase were modeled as linear elastic materials. The base was also given cross-anisotropic material properties. Use of an anisotropic characterization has been found to be necessary for correctly modeling the tension effect in the unstabilized granular bases (*15*). To model the tests, the wheel load was applied as a uniform pressure of 689 kPa (100 psi) over a circular area of radius 116 mm (4.55 in.) (Figure 1). A fixed boundary was assumed at the bottom of the 1118-mm (44-in.) thick subgrade where a concrete slab existed.

Linear elastic moduli used to model the cement-treated subbase were estimated from both charts and empirical correlations obtained from several sources (*16–20*). Resilient moduli in these correlations were related to the unconfined compressive strength of laboratory specimens prepared from cement-treated materials used in this study. For the soil-cement subbase of Section 11, the elastic moduli ranged from $3.5 * 10^3$ to $8.9 * 10^3$ MPa (507 to 1,300 ksi). Similarly, for the cement-stabilized crushed-stone subbase of Section 12, the moduli ranged from $8.3 * 10^3$ to $14.8 * 10^3$ MPa (1,200 to 2,000 ksi). After reviewing the variations in the moduli, a modulus of $4.14 * 10^3$ MPa (600 ksi) was assigned to the cement-treated silty sand subbase of Section 11, and $10.34 * 10^3$ MPa (1,500 ksi) to the cement-stabilized crushed-stone subbase of Section 12. The Poisson's ratio was assumed to be 0.2 for both sections (*20*).

The resilient modulus of the AC layer was taken (based on previous studies) to be $1.72 * 10^6$ kPa (250,000 psi) with a corresponding Poission's ratio of 0.35. To initiate the nonlinear analysis, initial estimates of the moduli must be input into the GT-PAVE program. The unstabilized crushed-stone bases were initially assigned vertical resilient moduli varying from 206,850 kPa (30 ksi) at the bottom to 413,700 kPa (60 ksi) at the top. The horizontal resilient moduli were taken to be 80 percent of the vertical moduli in the 203-mm (8-in.) thick anisotropic base. Similarly, an assumed Poisson's ratio of 0.43 in the vertical direction was reduced to 0.15 in the horizontal direction based on previous studies (*15*). After the first iteration of the first load increment, the material parameters of Uzan's model (Equation 1) were used for the nonlinear crushed-stone base. Material properties of the subgrade were modeled to be nonlinear isotropic as previously discussed, with a Poisson's ratio of 0.4. Initial moduli input to the program varied from 40 681 kPa (5900 psi) at the top to 103 425 kPa (15,000 psi) at the bottom of the subgrade.

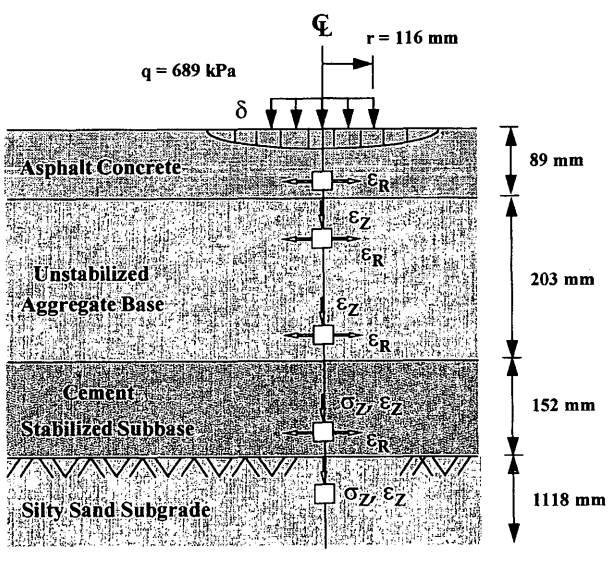

FIGURE 1 Typical cross section of inverted sections.

Table 4 compares the predicted GT-PAVE response variables with the measured ones. In general, finite-element predictions are in reasonably good agreement with the observed behavior of both inverted sections. Predictions were, however, in better agreement with observed response for Section 11 than for Section 12. The value of the vertical strain on top of the subgrade ($390 * 10^{-6}$ mm/mm) and the horizontal tensile strain at the bottom of the AC ($340 * 10^{-6}$ mm/mm) are essentially the same as the measured values in the cement-treated silty sand subbase (Section 11). In Section 12, the predicted value of the vertical stress on top of the subgrade [24.1 kPa (3.5 psi)] is in good agreement with the measured value of 23.4 kPa (3.4 psi). For this section, predicted tensile strain in the bottom of the AC was $340 * 10^{-6}$ mm/mm compared with a measured value of $260 * 10^{-6}$ mm/mm, which is still considered a reasonable prediction. Other predicted strains in this layer also differed from measured values in a similar manner. Strains in different layers are quite hard to predict with a high degree of accuracy.

The predictions summarized in Table 4 tend to verify the ability of nonlinear, anisotropic finite-element models such as GT-PAVE, to reasonably accurately predict a large number of measured stress, strain, and deflection response variables simultaneously. Such predictions are hard to achieve and indicate the model used is reasonably valid. This cannot be said for models that are verified by predicting only one or perhaps two measured response variables.

Figure 2 shows contours of horizontal radial stresses plotted on the top portion of the finite-element mesh for Section 12. The contours in Figure 2 show that the upper portion of the cement-treated subbase and almost all of the unstabilized crushed-stone base near the load are in horizontal compression. The bottom half of the subbase, as well as a thin layer on top of the subgrade, is in horizontal tension.

As a result of placing the cement-stabilized layer beneath the aggregate base, primarily horizontal compressive stresses of magnitudes ranging from 0 to 110 kPa (0 to 16 psi) are developed in the unstabilized crushed-stone base. This aggregate base performed well in the laboratory tests as indicated by the low measured permanent deformation (18 percent of total) and the high calculated values of resilient moduli (241 to 552 kPa; 35 to 80 ksi). Relatively high horizontal tensile stresses (up to 586 kPa; 85 psi under the load centerline) were predicted at the bottom of the stabilized subbase in Sections 11 and 12.

Sensitivity Analysis

A sensitivity analysis of inverted sections was performed using the GT-PAVE program for four different unstabilized aggregate base thicknesses varying from 76 to 406 mm (3 to 16 in.) and three different cement-treated subbase thicknesses varying from 102 to 254 mm (4 to 10 in.). The purpose of the sensitivity analysis was to find optimum design geometries for the inverted sections as defined by horizontal tensile strain in the bottom of the AC, vertical stress on the subgrade, and the tensile stress in the cement-stabilized subbase. Levels of subbase stabilization comparable to Section 11 and 12 were used corresponding to resilient moduli of $4.14 * 10^3$ MPa (600 ksi) and $10.34 * 10^3$ MPa (1,500 ksi), respectively. An impor-

TABLE 4 Comparison of Predicted and Measured Response Variables[1]

RESPONSE	TOP SUBGRADE		BOTTOM SUBBASE		BOTTOM BASE		TOP BASE	BOTTOM AC		SURFACE DEFLECTION		
	σ_z (kPa)	ε_z ($\frac{\mu m}{mm}$)	ε_R ($\frac{\mu m}{mm}$)	ε_z ($\frac{\mu m}{mm}$)	ε_R ($\frac{\mu m}{mm}$)	ε_z ($\frac{\mu m}{mm}$)	ε_z ($\frac{\mu m}{mm}$)	ε_R ($\frac{\mu m}{mm}$)	ε_z ($\frac{\mu m}{mm}$)	$\delta_{C.L.}$[2] (mm)	δ_{254}[3] (mm)	δ_{368}[3] (mm)
MEASURED (Section 11)	22.8	0.390	-	-	0.054	0.370	0.730	-0.340	-	0.48	0.18	0.08
PREDICTED (Section 11)	27.6	0.390	-0.079	0.045	0.051	0.317	1.050	-0.348	0.536	0.41	0.23	0.15
MEASURED (Section 12)	23.4	0.340	-	-	0.022	0.420	0.760	-0.260	-	0.41	0.15	0.08
PREDICTED (Section 12)	24.1	0.236	-0.046	0.025	0.035	0.362	1.047	-0.341	0.532	0.38	0.20	0.15

Notes: 1. A "-" in data field indicates no data was taken

2. Measured deflections at centerline $\delta_{C.L.}$ are extrapolated

3. Deflections measured at 254 mm and 368 mm radial distances away from centerline

4. 1 in = 25.4 mm; 1 psi = 6.895 kPa

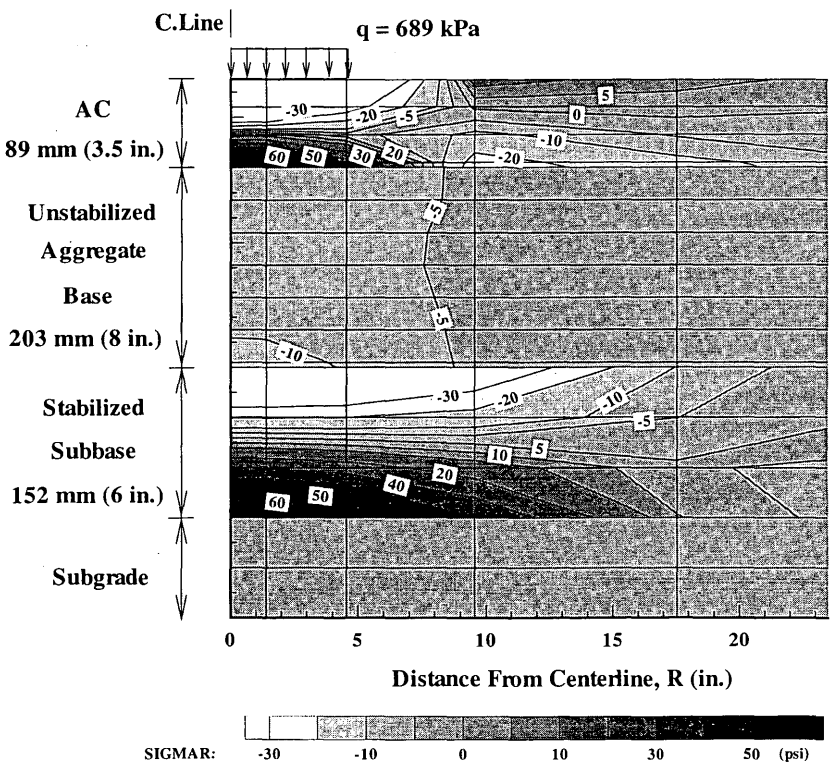

Notes: 1. 1 in. = 25.4 mm; 1 psi = 6.895 kPa

2. Tension is positive

FIGURE 2 Variation of radial tensile stresses throughout unstabilized aggregate base and cement stabilized subbase in Section 12.

tant factor in achieving good performance of an inverted section is to provide a subbase having sufficient strength to prevent fatigue- and durability-related failures.

The sensitivity analysis (Figure 3) indicates that increasing the thickness of the unstabilized aggregate base in the inverted sections causes an important increase in the horizontal strains at the bottom of the AC for stabilized subbase thicknesses of 102, 152, and 254 mm (4, 6, and 10 in.). Resilient surface deflections also increase with increasing base thickness although these results are not presented. For a base thickness equal to or greater than 152 mm, only a very small reduction occurs in the vertical subgrade stress with increasing base thickness (Figure 4). Therefore, inverted pavements having a 152-mm to 203-mm (6- to 8-in.) thick unstabilized crushed-stone base and also a similar thickness of cement-stabilized subbase appear to be a practical, economical design that minimizes tensile strain in the AC and vertical stress on the subgrade. Base or subbase thicknesses less than 152 mm (6 in.) are considered impractical to construct. This finding is in general agreement with the full-scale field tests recently conducted by North Carolina DOT.

Figure 5 shows the variation of horizontal radial tensile strain at the bottom of AC with increasing AC thicknesses for both inverted and conventional sections. The lower curve, which shows significant reductions in tensile strain compared to the conventional sections, is for inverted sections having a 152-mm (6-in.) thick base and subbase. For both sections, the horizontal radial tensile strain at the bottom of the AC decreases significantly with increasing AC thickness, suggesting the potential for improved fatigue life of the AC.

The variation of the horizontal radial tensile stress at the bottom of the stabilized subbase beneath the center of the load is shown in Figure 6 as a function of subbase thicknesses. In both the low-and high-moduli subbase inverted sections, an important decrease in tensile stress occurs with increasing subbase thickness. Fatigue life of the cement-stabilized subbase can therefore be improved by increasing subbase thickness.

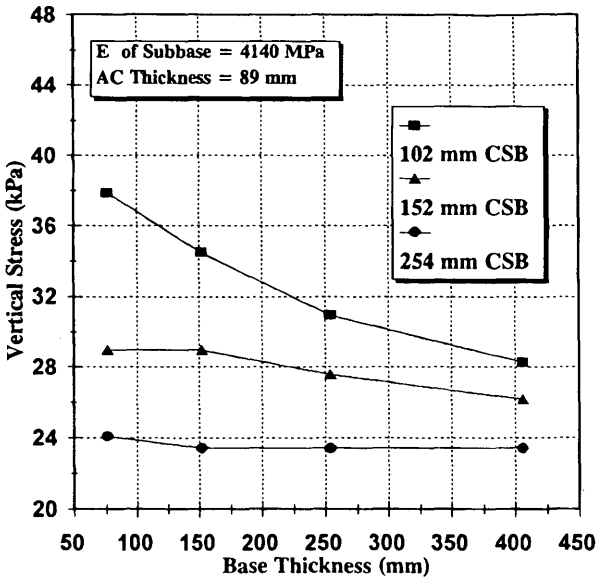

1. CSB: Cement Stabilized Subbase
1 in = 25.4 mm, 1 psi = 6.895 kPa

FIGURE 4 Variation of vertical stress on subgrade with base thickness in Section 11.

CONCLUSIONS

The full-scale test results show that cement-stabilized inverted sections having a subbase thickness of 152 to 203 mm (6 to 8 in.) can successfully withstand large numbers of heavy loadings better than both the conventional and full-depth AC sections used in this study. A full-depth AC section having better rut resistance would, of

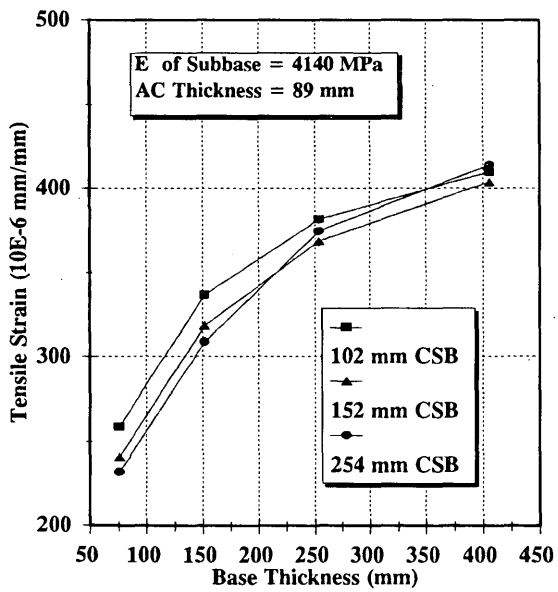

1. CSB: Cement Stabilized Subbase
1 in = 25.4 mm

FIGURE 3 Variation of horizontal tensile strain at bottom of AC with base thickness in Section 11.

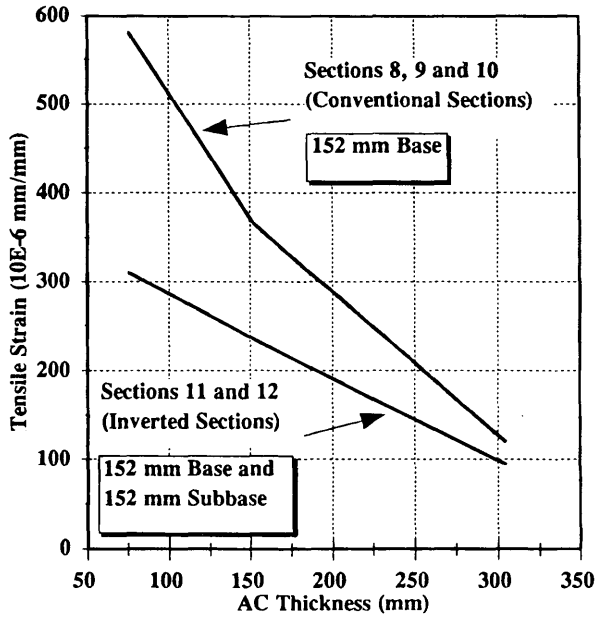

Note: 1 in = 25.4 mm

FIGURE 5 Variation of radial tensile strain at bottom of AC with AC thickness.

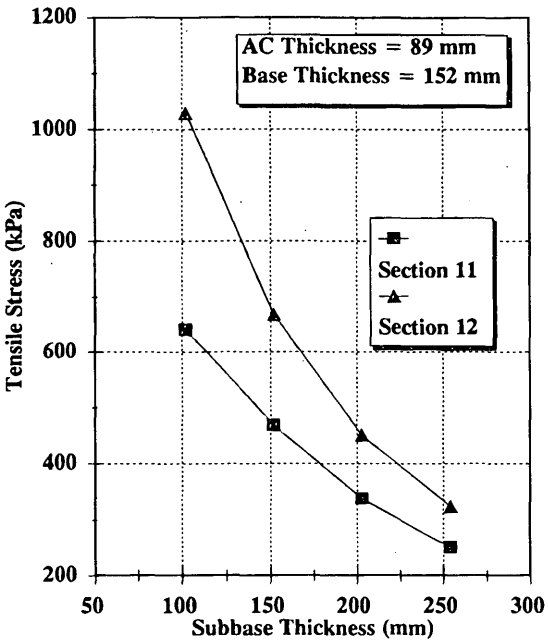

Note: 1 in = 25.4 mm, 1 psi =6.895 Kpa

FIGURE 6 Variation of radial tensile stress beneath centerline at bottom of cement stabilized subbase with subbase thickness.

course, perform better. The inverted sections also exhibit lower vertical stresses on the subgrade and lower resilient surface deflections than the other sections. The lower vertical stresses on the subgrade are caused primarily by the "beam" action of the stabilized subbase, which spreads the stress out. The significant reduction of vertical stress on the subgrade makes the use of an inverted section appealing for construction over a weak subgrade. The high-quality cement-stabilized crushed-stone subbase inverted section had the lowest tensile strain in the bottom of the AC of all 12 test sections studied. The low tensile strain in the AC and low vertical subgrade stress help explain why this section performed best.

Inverted sections make optimum use of the excellent compressive characteristics of unstabilized aggregate by placing it above the cement-stabilized layer where radial stresses are compressive. Better compaction of unstabilized materials placed over the stabilized layers is achieved. As a result of better confinement and a higher level of compaction, permanent deformations in the base are small. Reflection cracking is significantly reduced or eliminated since the cement-treated layer is placed deep in the section below the aggregate base.

Pavement response predictions for the two inverted sections made at six locations were in reasonably good agreement with observed values. This finding indicates the GT-PAVE nonlinear, cross-anisotropic program and the material characterization models used were valid. The theoretical sensitivity analysis performed using these models indicate an optimum and economical inverted pavement design placed on a weak to moderately strong subgrade would have an unstabilized aggregate base 152 mm (6 in.) thick and a 152-mm to 203-mm (6- to 8-in.) thick cement-stabilized subbase.

REFERENCES

1. *Highway Statistics, 1990.* FHWA U.S. Government Printing Office, Washington, D.C. 1990.
2. Johnson, V. W. Comparative Studies of Combinations of Treated and Untreated Bases and Subbases for Flexible Pavements. *Bulletin 289,* HRB, National Research Council, Washington, D.C., 1960, pp. 44–61.
3. McGhee, K. H. *Pavement Design Performance Studies.* Final Report on Phase C Research Report BHRC 70-R44, Virginia Council, 1971.
4. Grau, R. W. *Evaluation of Structural Layers of Flexible Pavements.* Miscellaneous Paper S-73-26. Waterways Experiment Station, 1973.
5. Tayabji, S. D., P. J. Nussbaum, and A. T. Ciolko. Evaluation of Heavily Loaded Cement Stabilized Bases. In *Transportation Research Record 839,* TRB, National Research Council, Washington, D.C., 1982, pp. 6–11.
6. Maree, J. H., N. J. W., van Zyl, and C. R. Freeme. Effective Moduli and Stress Dependence of Pavement Materials as Measured in Some Heavy-Vehicle Simulator Tests. In *Transportation Research Record 852,* TRB, National Research Council, Washington, D.C., 1982.
7. Maree, J. H., C. R. Freeme, N. J. W. van Zyl, and P. F. Savage. The Permanent Deformation of Pavements With Untreated Crushed-Stone Bases as Measured in Heavy Vehicle Simulator Tests. *Proc. 11th Australian Road Research Board Conference,* Melbourne, 1982.
8. O'Neil, D. J., J. P. Mahoney, and N. C. Jackson. *An Evaluation of Granular Overlays in Washington State.* Final Technical Report, Report No. FHWA-SA-92-042. Washington State Department of Transportation, 1992.
9. Horak, E., J. C. du Pisani, and C. J. van der Merwe. Rehabilitation Alternatives for Typical "Orange Free State" Rural Roads. *Proc. Annual Transportation Convention,* National Institute for Transport and Road Research, Perth, Australia, 1986.
10. Alba, J. L. *Laboratory Determination of Resilient Modulus of Granular Materials for Flexible Pavement Design.* Ph.D. dissertation. Georgia Institute of Technology, Atlanta, 1993.
11. Uzan, J. Characterization of Granular Materials. In *Transportation Research Record 1022,* TRB, National Research Council, Washington, D.C., 1985, pp. 52–59.
12. Barksdale, R. D., and H. A., Todres. *A Study of Factors Affecting Crushed Stone Base Performance.* Report SCEGIT-82-109, Georgia Institute of Technology, Atlanta, 1983.
13. Barksdale, R. D. Crushed Stone Base Performance. In *Transportation Research Record 954,* TRB, National Research Council, Washington, D.C., 1984, pp. 78–87.
14. Zienkiewicz, O. C., Y. K. Cheung, and K. G. Stagg. Stress Analysis of Rock as a "No Tension" Material. *Geotechnique,* Vol. 18, 1968, pp. 56–66.
15. Barksdale, R. D., S. F. Brown, and F. Chan. *NCHRP Report 315: Potential Benefits of Geosynthetics in Flexible Pavements.* TRB, National Research Council, Washington, D.C., 1989.
16. Felt, E. J., and M. S. Abrams. Strength and Elastic Properties of Compacted Soil-Cement Mixtures. *ASTM Special Technical Publication,* No. 206, 1957, pp. 152–173.
17. Jones, R. Measurement of Elastic and Strength Properties of Cemented Materials in Road Bases. In *Highway Research Record 128,* HRB, National Research Council, Washington, D.C., 1966, pp. 101–111.
18. Williams, R. I. T. Properties of Cement Stabilized Materials. *The Journal of the Institution of Highway Engineers,* Vol. 19, No. 2, 1972, pp. 5–19.
19. Hadley, O. W. Material Characterization and Inherent Variation Analysis of Soil-Cement Field Cores. In *Transportation Research Record 1295,* TRB, National Research Council, Washington, D.C., 1991, pp. 23–36.
20. *Soil Stabilization In Pavement Structures—A User's Manual.* Vol. 1 and 2. Report FHWA-IP-80-2. Office of Development Implementation Division, FHWA, U.S. Department of Transportation, 1979.

Publication of this paper sponsored by Committee on Flexible Pavement Design.